

Orientation-Dependent Entanglement Lifetime in a Squeezed Atomic Clock

Ian D. Leroux, Monika H. Schleier-Smith, and Vladan Vuletić

*Department of Physics, MIT-Harvard Center for Ultracold Atoms and Research Laboratory of Electronics,
Massachusetts Institute of Technology, Cambridge, Massachusetts 02139, USA*

(Received 23 March 2010; published 25 June 2010)

We study experimentally the application of a class of entangled states, squeezed spin states, to the improvement of atomic-clock precision. In the presence of anisotropic noise, the entanglement lifetime is strongly dependent on squeezing orientation. We measure the Allan deviation spectrum of a clock operated with a phase-squeezed input state. For averaging times up to 50 s the squeezed clock achieves a given precision 2.8(3) times faster than a clock operating at the standard quantum limit.

DOI: 10.1103/PhysRevLett.104.250801

PACS numbers: 06.30.Ft, 06.20.-f, 42.50.Dv, 42.50.Lc

Atomic interference provides an exquisitely sensitive tool for measuring gravitation, magnetic fields, acceleration, rotation, and time itself [1,2]. Quantum-mechanical entanglement may enhance the precision of such measurements: maximally entangled states can increase the sensitivity of the interference fringe to the parameter of interest [3], while squeezed spin states can redistribute quantum noise away from it [4,5]. In experiments, both approaches have overcome the standard quantum limit (SQL) of phase sensitivity [6–13]. However, Huelga *et al.* pointed out early on that entangled states might provide little gain in metrological performance because they are more fragile than uncorrelated states, such that the entanglement-induced increase in phase sensitivity comes at the expense of reduced interrogation time [14]. Nonetheless, analyses with specific noise models [15,16] found regimes where entanglement can improve metrological performance despite decoherence. It is thus interesting, practically as well as fundamentally, to investigate the lifetime of the entangled states relevant to metrology.

In this Letter we present an atomic clock whose precision exceeds the SQL thanks to a phase-squeezed input state, as also recently demonstrated by Louchet-Chauvet *et al.* [11]. We show the first measurement of such a clock's Allan deviation spectrum, indicating that the clock reaches a given precision 2.8(3) times faster than the SQL for averaging times up to 50 s. We demonstrate that for a clock in which the dominant environmental perturbation is atomic frequency noise, the entanglement lifetime varies by an order of magnitude depending on whether the squeezed variable is the phase (subject to environmental perturbation) or the (essentially unperturbed) population difference between states. The squeezed states are prepared by cavity feedback squeezing [10,17], a new technique which deterministically produces entangled states of distant atoms using their collective interaction with an optical resonator.

Given any two-level atom we define a (pseudo)spin-1/2 s_i . For an ensemble of such atoms, we introduce the total spin $\mathbf{S} = \sum s_i$ whose S_z component and azimuthal angle ϕ

represent the population difference and relative phase, respectively, between the atomic levels. Preparing all the atoms in the same single-particle quantum state places the ensemble in a coherent spin state (CSS) where the variance of spin components perpendicular to the mean spin is given by $|\langle \mathbf{S} \rangle|/2$ [18]. While decoherence can shorten $|\langle \mathbf{S} \rangle|$ and reduce this variance, only entanglement between atoms can improve the signal-to-noise ratio in a measurement of the orientation of \mathbf{S} [4,5]. We quantify the signal by a contrast $C = |\langle \mathbf{S} \rangle|/S_0$, where S_0 is the maximum spin length for a system with $2S_0$ total atoms. We also introduce C_{in} , the similarly defined contrast for the uncorrelated state before the squeezing procedure. We can now define a metrological squeezing parameter [4] $\zeta = 2\Delta S_{\perp}^2 C_{\text{in}} / (S_0 C^2)$ which compares the squared signal-to-noise ratio for the best possible measurement on a CSS with the initially available spin length $C_{\text{in}} S_0$ to that of the actual measurement with transverse variance ΔS_{\perp}^2 and spin length $C S_0$. If $\zeta < 1$, the total spin orientation is more precisely determined, in some plane, than would be possible if $2C S_0$ atoms were uncorrelated [19].

If we prepare a CSS in the equatorial plane, we expect that the phase noise will increase at long times due to classical fluctuations in our apparatus of the energy difference between levels [Fig. 1(c), top]. As discussed below, this broadening becomes noticeable in our system within 1 ms. In the number direction, the primary mechanism that increases polar angle uncertainty $\Delta S_z / |\langle \mathbf{S} \rangle|$ is loss of contrast (reduction in the length of the mean spin vector $|\langle \mathbf{S} \rangle|$), which occurs on a longer time scale $T_{\text{coh}} = 11(1)$ ms in our apparatus. A phase-squeezed state will therefore suffer much more rapid broadening of its narrow axis [Fig. 1(c), middle] than will a number-squeezed state [Fig. 1(c), bottom]. Intriguingly, a number-squeezed state is less vulnerable to phase noise than an uncorrelated state: an increase in phase variance by several times the width of the original CSS might still be small compared to the anti-squeezed phase variance of the number-squeezed state.

We work with laser-cooled ^{87}Rb and use the canonical magnetic-field-insensitive clock transition between

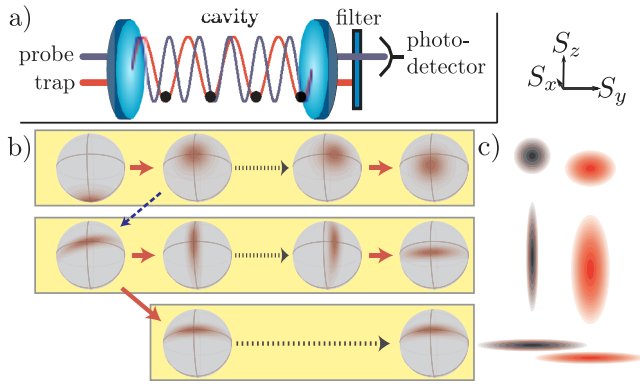


FIG. 1 (color online). (a) Setup: A standing-wave dipole potential confines ^{87}Rb atoms within an optical resonator where they interact with probe light via their state-dependent index of refraction. The probe light is used for cavity feedback squeezing [10,17] and final state readout. (b) Pulse sequences: A standard Ramsey protocol (top bar) consists of optical pumping into the spin-down CSS, rotation about S_y into the equatorial plane using a microwave pulse (solid red arrow), free precession time (dotted black arrow), and conversion of the accrued phase into a measurable population difference by a rotation about S_x . We can shear the CSS into a squeezed state using cavity feedback (dashed blue arrow), then orient the narrow axis of the squeezed state in the phase direction (middle bar) or in the S_z direction (bottom bar). (c) Effect of phase noise: The ideal CSS (shown schematically at top left) is perturbed by classical phase fluctuations accrued during the free precession, increasing its variance in one direction (top right). The same fluctuations are detrimental to phase-squeezed states (middle row) but much less noticeable in number-squeezed states (bottom). The broadened distributions are offset vertically and horizontally in the figure to avoid overlap.

$|F = 1, m_F = 0\rangle$ and $|F = 2, m_F = 0\rangle$ in the electronic ground state $5^2S_{1/2}$. The atomic cloud is held by a far-detuned dipole trap inside a Fabry-Pérot resonator with a finesse of $5.6(2) \times 10^3$ and a free spectral range of 5632(1) MHz [Fig. 1(a)]. One resonator mode, used for probing, is detuned halfway between the D_2 optical transitions for the two clock states. The total spin S corresponds to a sum over the atomic cloud, weighted by the atoms' position-dependent coupling to the resonator mode so as to yield an effective uniform-coupling description [8,10]. The atomic index of refraction shifts the cavity resonance frequency by equal and opposite amounts for atoms in each of the two clock states, the net shift being proportional to their population difference $2S_z$. In order to read out the atomic state, the resonator is driven by probe light tuned to the slope of the cavity resonance, so that atom-induced shifts of the resonance frequency are revealed as changes in the transmitted fraction of probe light, which we detect on an avalanche photodiode. The probe light is a sideband modulated at 36 GHz onto a laser that is locked to a far-detuned cavity mode [8]. A 2.4 G bias field along the cavity axis combined with circular trap polarization keeps the clock frequency independent of trap

power to first order [8], but makes it linearly sensitive to magnetic-field fluctuations with a coefficient of 3.7 kHz/G. These fluctuations are the dominant noise affecting the clock spin. Aside from the choice of lock detuning, bias field, and trap polarization given above, the details of our apparatus are the same as in Refs. [8,10].

Arbitrary rotations of the spin vector are performed using resonant microwave pulses, while squeezing the uncertainty region requires an effective interaction between the atoms which we generate by cavity feedback, exploiting their common coupling to the light field of the resonator [10,17]. As the atomic index of refraction shifts the cavity resonance by an amount proportional to S_z , it changes the intracavity intensity of probe light. The probe imparts a light shift to the atoms, each of which thus acquires a phase shift which depends on the state of all other atoms in the ensemble, thus introducing the correlations necessary for squeezing. The S_z -dependent phase shift shears the circular uncertainty region of the CSS into an ellipse with its long (antisqueezed) axis oriented at a small and known angle to the equatorial plane [Fig. 1(b), middle bar]. Note that, due to photon shot noise in the probe light, the states thus prepared are actually mixed states with an area much larger than is required by the Heisenberg uncertainty relations [17].

To measure the lifetime of a phase-squeezed state, we load the dipole trap with an ensemble of atoms collected in a magneto-optical trap, prepare a CSS by optically pumping the atoms into the $|F = 1, m_F = 0\rangle$ state, and then apply a microwave $\pi/2$ pulse to rotate it into the equatorial plane of the Bloch sphere [10]. We typically work with $2S_0 \approx 3 \times 10^4$ effective atoms and an initial contrast $C_{\text{in}} = 90(2)\%$, yielding a projection-noise-limited phase uncertainty of ~ 6 mrad [4]. Cavity feedback squeezing with a pair of weak probe pulses then drives the atoms into a state with $\zeta^{-1} \approx 4$ dB. A rotation of nearly $\pi/2$ converts this into a phase-squeezed state. After allowing the spins to precess for a variable time T_R , the phase information is converted back to a population difference with a final $\pi/2$ pulse and read out by observing the transmission of a pair of strong probe pulses. We apply the probe light in paired pulses, separated by a π pulse (spin echo), to suppress inhomogeneous light shifts and technical noise.

This sequence of operations constitutes a Ramsey-type atomic clock with a squeezed input state. We perform 10 sequences of state preparation, precession, and readout for each sample of atoms loaded from the magneto-optical trap, and the entire experimental cycle repeats every 9 seconds. We measure the phase variance of the CSS using the same experimental sequence but without the squeezing probe pulses. To measure the lifetime of a number-squeezed state, we rotate the sheared state slightly to orient its narrow axis along S_z and then simply hold it for a time T_R before reading it out [Fig. 1(b), bottom bar]. In all three cases, comparing the normalized variance to the squared contrast for the readout signal yields the metrological squeezing parameter ζ , which we plot in Fig. 2. The SQL

(black solid line at $\zeta = 1$) is calculated from independent absolute atom number measurements based on precisely measured cavity parameters, and verified experimentally as in Ref. [8].

We first use the CSS to evaluate the classical phase noise (Fig. 2, black solid circles). The data are well described by the model $\zeta(T_R) = \zeta(0) + 2S_0 C_{\text{in}} \Delta\omega^2 T_R^2$ (dotted fit), involving an initial angular uncertainty described by $\zeta(0)$ and additional fluctuations of the transition frequency between measurements with variance $\Delta\omega^2$. After a precession time of $700 \mu\text{s}$, the effect of the classical noise $\Delta\omega = 2\pi \times 1.3 \text{ Hz}$ exceeds the initial projection noise, and the phase variance increases quadratically thereafter. Note that reaching the SQL in an atomic clock requires not only projection-noise-limited state preparation and readout, but also an interrogation time short enough that quantum projection noise remains the dominant uncertainty on the clock signal.

The same model yields a good description of the behavior of a phase-squeezed state (red solid squares and dashed line). We initially observe a reduced phase variance $\zeta(0) < 1$, as expected. The same frequency noise $\Delta\omega$ (constrained in the fit) broadens the phase-squeezed state sooner than the CSS because there is less quantum noise to mask the classical fluctuations. Nevertheless, the state only ceases to be squeezed [$\zeta(t) = 1$] at a time $t = T_{\text{sq}} \approx 600 \mu\text{s}$ which approaches the squeezing-independent bound $T_{\text{sq}} < (\sqrt{2S_0 C_{\text{in}}} \Delta\omega)^{-1} \approx 700 \mu\text{s}$ set by the classical broadening. Even when ζ reaches 1, the initial squeezing still

improves the signal-to-noise ratio by $\approx 3 \text{ dB}$ over that of an initially unsqueezed state, which has also suffered the same classical broadening.

Matters are very different when we prepare a number-squeezed state and read out its reduced S_z variance directly after a hold time T_R (Fig. 2, open green circles). Instead of operating a clock, which measures the evolution of the phase angle, we are now examining the evolution of the polar angle corresponding to the population difference between clock states. Frequency noise adds no uncertainty to this spin component, so ζ can remain below unity (squeezed) for 5 ms, 8 times longer than for the phase-squeezed state, until dephasing between the atoms, visible as loss of signal contrast (Fig. 2, inset), creates a mixed state that is no longer sufficiently entangled to overcome the SQL. We also measure the phase variance of the number-squeezed state by applying a $\pi/2$ pulse just before readout and see no change out to 5 ms (not shown); the classical frequency noise is entirely hidden by the anti-squeezed initial phase variance.

Since the decay of the phase-squeezed state results from classical frequency noise, it can be suppressed by standard techniques. For example, we have operated a ‘‘clock’’ sequence with a phase-squeezed input state, but with an additional spin-echo π pulse halfway through the precession time. The final phase is then insensitive to the atomic transition frequency, which protects the state from slow frequency fluctuations but makes it useless for time keeping. The state remains squeezed 2 ms after being prepared in the otherwise fragile phase-squeezed orientation (Fig. 2, open blue squares).

As a demonstration, we have operated a fully functional squeezed clock with a Ramsey interrogation time $T_R = 200 \mu\text{s}$, short enough that the classical frequency noise in our system does not destroy the phase squeezing. The effective atom number was $2S_0 = 3.5 \times 10^4$, the clock cycle time was $T_c = 9 \text{ s}$, and the signal contrast was $C = 81\%$. A single Ramsey interrogation was performed for each magneto-optical trap loading cycle, giving a duty factor of 2×10^{-5} . The result is the first measurement of Allan deviation [20] for an atomic clock operating beyond the SQL, including all noise and slow drifts (Fig. 3, red solid line). For comparison, we also evaluate a clock operated with an uncorrelated input state close to a CSS, 100(2)% signal contrast, and otherwise identical parameters (Fig. 3, black circles). An ideal projection-noise-limited clock with the same atom number, interrogation time, and duty factor could reach a stability [21]

$$\sigma_{\text{SQL}}(\tau) = \frac{1}{\omega_0 T_R} \sqrt{\frac{T_c}{2S_0 \tau}} = 1.85 \times 10^{-9} \text{ s}^{1/2} / \sqrt{\tau}$$

(Fig. 3, dashed black line), where $\omega_0 = 2\pi \times 6.83 \text{ GHz}$ is the clock transition frequency. At short times our squeezed clock reaches a fractional frequency stability of $\sigma(\tau) = 1.1 \times 10^{-9} \text{ s}^{1/2} / \sqrt{\tau}$, a factor of 2.8(3) in variance below the SQL. At longer times we reach a noise floor at 10^{-10}

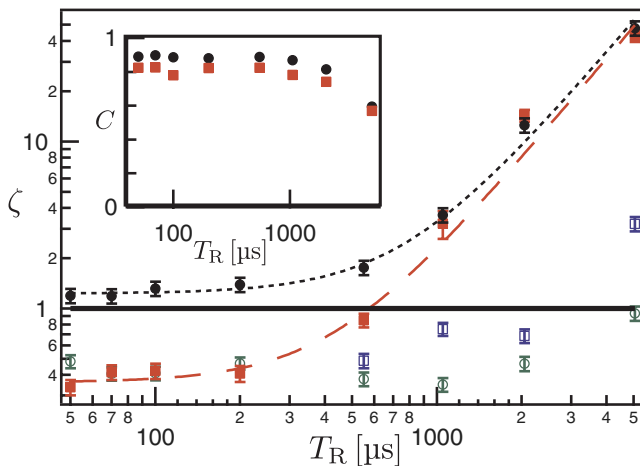


FIG. 2 (color online). Metrological squeezing parameter ζ as a function of time. The phase variance for an initial CSS (black solid circles, dotted line) or phase-squeezed state (red solid squares, dashed line) increases due to classical frequency noise. The number variance of a number-squeezed state (green open circles) or the phase variance of a phase-squeezed state protected by a spin echo (blue open squares) can remain below the SQL (solid black line) substantially longer. Error bars show the statistical uncertainty of the variance determination. Inset: Signal contrast C for the CSS (black solid circles) and squeezed states (red solid squares).

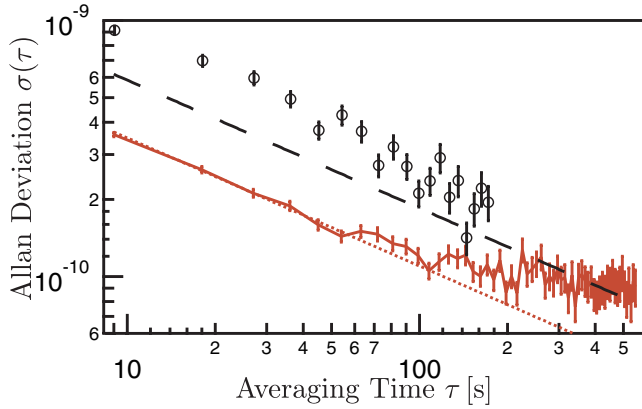


FIG. 3 (color online). Allan deviation of a squeezed clock operating below the SQL. The solid red line with error bars was measured using a squeezed input state. The dotted red line indicates $\sigma(\tau) = 1.1 \times 10^{-9} \text{ s}^{1/2}/\sqrt{\tau}$. The open black circles were measured with a traditional clock using an uncorrelated input state. The dashed black line at $1.85 \times 10^{-9} \text{ s}^{1/2}/\sqrt{\tau}$ indicates the SQL.

fractional stability (0.7 Hz absolute stability) due to slow drifts of the magnetic field in our apparatus.

The performance of our clock benefits from squeezing because we impose the constraint of a short Ramsey precession time. For long interrogation times the classical noise dominates the initial phase noise and our clock is not projection-noise limited. External constraints on the interrogation time do, however, occur in practice. For instance, the precession time in optical frequency standards is typically limited by dephasing of the local oscillator laser, not atomic decoherence, so that their performance could be improved by the use of squeezed input states [15,16].

The phase noise of our squeezed clock (≈ 3 mrad) is already close to that of state-of-the-art fountain clocks [2], whose SQL is ≈ 1 mrad. Our frequency stability is comparatively poor only because this phase uncertainty is divided by a much shorter Ramsey precession time (200 μs instead of ~ 1 s). If the classical frequency noise in our clock could be controlled at the level of ~ 100 μHz , perhaps by replacing the dipole trap with a magnetic trap at the magic bias field of 3.23 G, the squeezed lifetime could be extended sufficiently to allow a Ramsey precession time of 1 s, as demonstrated by Treutlein *et al.* on an atom chip similar to the one used in the present experiment [22]. Even without improvements to our squeezed-state preparation or 9 s cycle time [23], this could yield a short-term instability of $\sigma(\tau) \approx 2 \times 10^{-13} \text{ s}^{1/2}/\sqrt{\tau}$, within an order of magnitude of the instability of current fountain clocks [2].

This work was supported in part by the NSF, DARPA, and the NSF Center for Ultracold Atoms. M.H.S. acknowledges support from the Hertz Foundation and NSF. I.D.L. acknowledges support from NSERC.

- [1] A. D. Cronin, J. Schmiedmayer, and D. E. Pritchard, *Rev. Mod. Phys.* **81**, 1051 (2009).
- [2] S. Bize *et al.*, *J. Phys. B* **38**, S449 (2005).
- [3] J. J. Bollinger, W. M. Itano, D. J. Wineland, and D. J. Heinzen, *Phys. Rev. A* **54**, R4649 (1996).
- [4] D. J. Wineland, J. J. Bollinger, W. M. Itano, F. L. Moore, and D. J. Heinzen, *Phys. Rev. A* **46**, R6797 (1992).
- [5] D. J. Wineland, J. J. Bollinger, W. M. Itano, and D. J. Heinzen, *Phys. Rev. A* **50**, R67 (1994).
- [6] V. Meyer, M. A. Rowe, D. Kielpinski, C. A. Sackett, W. M. Itano, C. Monroe, and D. J. Wineland, *Phys. Rev. Lett.* **86**, 5870 (2001).
- [7] D. Leibfried, M. D. Barrett, T. Schaetz, J. Britton, J. Chiaverini, W. M. Itano, J. D. Jost, C. Langer, and D. J. Wineland, *Science* **304**, 1476 (2004).
- [8] M. H. Schleier-Smith, I. D. Leroux, and V. Vuletić, *Phys. Rev. Lett.* **104**, 073604 (2010).
- [9] J. Appel, P. J. Windpassinger, D. Oblak, U. B. Hoff, N. Kjørgaard, and E. S. Polzik, *Proc. Natl. Acad. Sci. U.S.A.* **106**, 10960 (2009).
- [10] I. D. Leroux, M. H. Schleier-Smith, and V. Vuletić, *Phys. Rev. Lett.* **104**, 073602 (2010).
- [11] A. Louchet-Chauvet, J. Appel, J. J. Renema, D. Oblak, and E. S. Polzik, arXiv:0912.3895.
- [12] C. Gross, T. Zibold, E. Nicklas, J. Estève, and M. K. Oberthaler, *Nature (London)* **464**, 1165 (2010).
- [13] M. F. Riedel, P. Böhi, Y. Li, T. W. Hänsch, A. Sinatra, and P. Treutlein, *Nature (London)* **464**, 1170 (2010).
- [14] S. F. Huelga, C. Macchiavello, T. Pellizzari, A. K. Ekert, M. B. Plenio, and J. I. Cirac, *Phys. Rev. Lett.* **79**, 3865 (1997).
- [15] D. J. Wineland, C. Monroe, W. M. Itano, D. Leibfried, B. E. King, and D. M. Meekhof, *J. Res. Natl. Inst. Stand. Technol.* **103**, 259 (1998).
- [16] A. André, A. S. Sørensen, and M. D. Lukin, *Phys. Rev. Lett.* **92**, 230801 (2004).
- [17] M. H. Schleier-Smith, I. D. Leroux, and V. Vuletić, *Phys. Rev. A* **81**, 021804(R) (2010).
- [18] M. Kitagawa and M. Ueda, *Phys. Rev. A* **47**, 5138 (1993).
- [19] A. S. Sørensen and K. Mølmer, *Phys. Rev. Lett.* **86**, 4431 (2001).
- [20] J. Vanier and C. Audoin, *The Quantum Physics of Atomic Frequency Standards* (Bristol, Philadelphia, 1989).
- [21] G. Santarelli, P. Laurent, P. Lemonde, A. Clairon, A. G. Mann, S. Chang, A. N. Luiten, and C. Salomon, *Phys. Rev. Lett.* **82**, 4619 (1999).
- [22] P. Treutlein, P. Hommelhoff, T. Steinmetz, T. W. Hänsch, and J. Reichel, *Phys. Rev. Lett.* **92**, 203005 (2004).
- [23] J. Lodewyck, P. G. Westergaard, and P. Lemonde, *Phys. Rev. A* **79**, 061401(R) (2009).